Symposium of the International Society for Rock Mechanics

Hydraulic Fracture Propagation under Varying In-Situ Stress Conditions of Reservoirs

P.L.P. Wasantha*, H. Konietzky

Geotechnical Institute, TU Bergakademie Freiberg, Gustav-Zeuner-Str. 1, Freiberg 09596, Germany

Abstract

In-situ stress state in deep reservoirs is highly variable due to many factors and it markedly influence the propagation behavior of hydraulic fractures. The direction and extent of hydraulic fracture propagation are predominantly controlled by the in-situ stress state of reservoirs. We conducted distinct element method-based numerical simulations to explore the behavior of hydraulic fracture propagation and containment under varying in-situ stress conditions and fluid injection rates. The results revealed that even a small contrast of minor principal stress between pay-zone and adjacent bounding zones can cause a significant hydraulic fracture containment. Simulations performed under different injection rates showed that the hydraulic fracture containment is also influenced by the injection rate and higher injection rates tend to increase the hydraulic fracture penetration into the adjacent bounding zones. Overall, the results of the present study generally suggest that the fracture propagation during hydraulic fracturing is not an unconstrained event as one would imagine and natural barriers such as varying in-situ stresses, which are common in deep reservoirs, often limit fracture propagation to a certain finite extent. In addition, operational conditions such as fluid injection rate can be selected appropriately to control the hydraulic fracture propagation into unproductive bounding strata.

1. Introduction

Hydraulic fracturing is used to enhance oil and gas recovery from unconventional reservoirs since few decades ago. The same technique is also used in applications such as geothermal energy extraction, CO_2 geo-sequestration

---

* Corresponding author. Tel.: +49-15206033870; fax: +49-3731 39-3638.
E-mail address: wasantha.liyanage@extern.tu-freiberg.de

and management of high stresses encountered with deep mining [1]. The direction and extent of hydraulic fracture propagation play important roles in the economics of oil and gas production projects. Therefore, a thorough understanding of the geometrical nature of hydraulic fracture propagation under reservoir conditions is imperative for successful hydraulic stimulation designs.

In-situ stress field in deep reservoirs is highly variable in nature. This cannot be explained by the effects of gravity and topography alone, for which the role of tectonic stresses is undeniable [2]. The state of the in-situ stress is one of the primary factors to be considered in design and implementation of hydraulic fracturing treatments [3, 4, 5]. Two fracture propagation models have been widely used for hydraulic stimulation designs of oil and gas reservoirs – (1) KGD model [6, 7] and (2) PKN model [8, 9]. Each model was developed based on different simplified assumptions and with certain limitations meaning that the user should carefully apply them with a sound understanding of these stipulated conditions. PKN model assumes an elliptical fracture cross section in the vertical plane and the formation stiffness is concentrated in the vertical planes perpendicular to the direction of fracture propagation while KGD model assumes a rectangular cross section in the vertical plane and the stiffness of the formation is concentrated in the horizontal plane [10]. The numerical simulation program of this study is compatible with the assumptions of the KGD model and thus further discussions are only limited to the KGD model. As Meyer [11] states, for a hydraulic fracture with unit height, the fracture length (l_t) and aperture width at the wellbore (w_t) can be expressed as shown in Equations 1 and 2, respectively, assuming zero leak-off into the formation (see Figure 1).

$$l_t = a \left[\frac{Q^3 G}{(1-\nu)\mu} \right]^{\frac{1}{6}} t^{\frac{2}{3}} \tag{1}$$

$$w_t = b \left[\frac{Q^3 (1-\nu)\mu}{G} \right]^{\frac{1}{6}} t^{\frac{1}{3}} \tag{2}$$

where, Q is the constant injection rate, G is the shear modulus, ν is the Poisson's ratio, μ is the viscosity of the fluid, t is the time and a, b are constants.
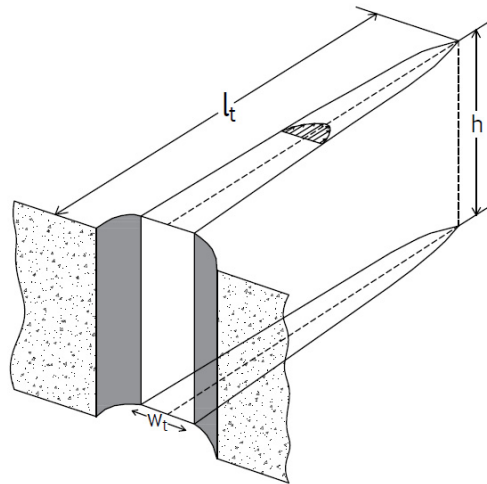

Fig. 1. KGD constant height fracture model (modified after [12]).

According to Meyer [11] and Geertsma and Haafkens [13], for a hydraulic fracture that propagates along both directions from a wellbore a is 0.48 and b is 1.32, and for a hydraulic fracture that propagates only along one

direction from the wellbore a is 0.68 and b is 1.87 (note that Q used in Equations 1 and 2 is the full injection rate applied to the wellbore).

It should be noted that both the PKN and KGD models assume the far field stress perpendicular to the fracture propagation direction (i.e. minor principal stress) is constant throughout the length of the hydraulic fracture.

Simonson et al. [14] considered a situation where the hydraulic fracture propagates into zones adjacent to the pay-zone in which the tectonic stresses are different (Figure 2). Based on the linear elastic fracture mechanics and assuming symmetric stress distribution (i.e. stresses above and below the pay-zone are equal) these researchers deduced the relationship shown in Equation 3 combining stress-intensity factor (K_I), stress contrast and fracture geometry (note that this relationship does not take the material property difference between the pay zone and bounding zone materials into account).
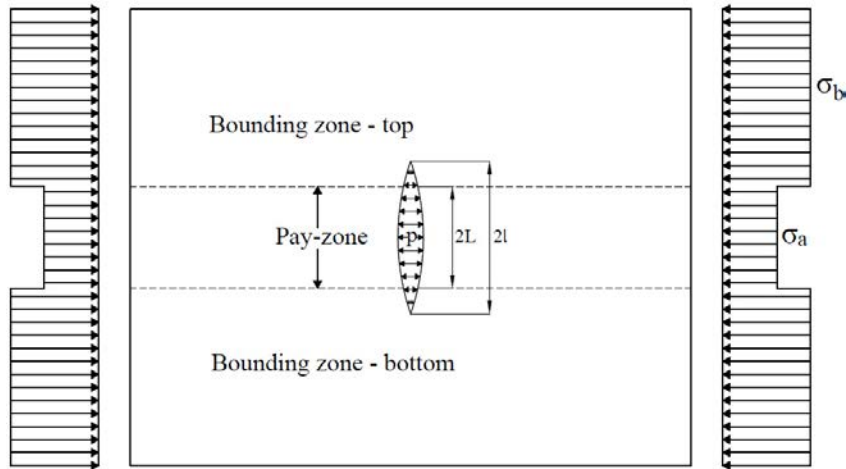

Fig. 2. Schematic diagram of the hydraulic fracture propagation under varying minor principal stress conditions (modified after [14]).

$$K_I = (\sigma_b - \sigma_a)\sqrt{\frac{l}{\pi}}\left\{2\sin^{-1}\left(\frac{L}{l}\right)\right\} + (p - \sigma_b)\sqrt{\pi l} \tag{3}$$

Extensive fracture propagation into the bounding zones can be expected if $\sigma_b < \sigma_a$ due to the required less pressure to propagate the hydraulic fracture into these regions compared to the pay-zone.

Although varying in-situ stress conditions can often be found in the field there have been only limited number of studies in the literature that investigated its influence on hydraulic fracture propagation and containment. In this paper, we qualitatively investigate this issue to reveal some critical insights of the underlying mechanisms using a numerical simulation program. Furthermore, we explore the effect of fluid injection rate on the hydraulic fracture containment under varying in-situ stress conditions such that the results can be used to optimize the operational conditions to achieve improved productivity.

2. Numerical simulation program

We used the distinct element method-based two-dimensional software Universal Distinct Element Code (UDEC) for the numerical simulation. The simulation program was systematically structured such that initially uniform minor principal stress (i.e. $\sigma_b = \sigma_a$) was applied and simulated fracture propagation geometry was compared with those predicted by the KGD fracture model (i.e. Equations 1 and 2) followed by the simulations under varying minor principal stresses (i.e. under different σ_a and σ_b values) and injection rates.

In case of the uniform in-situ stresses, a 1000m x 1000m model was first created and a major principal stress of 160 MPa and minor principal stress of 80 MPa were applied on the vertical and horizontal boundaries of the model, respectively. A joint was embedded in the center of the model parallel to the major principal stress direction for the hydraulic fracture propagation as the blocks in UDEC can only be made deformable and are indivisible. Properties used for the block material, embedded joint (i.e. hydraulic fracture) and the fracturing fluid are shown in Table 1. Fluid was injected at a constant rate (0.0833 m^3/s) to the domain nearest to the center of the model (i.e. the center of the embedded joint) for 100 seconds. The length and width (at the injection point) of the propagating hydraulic fracture against the injection time were recorded and compared with the corresponding variations predicted by the KGD fracture model.

After the model validation, the second series of simulations was conducted. The same model dimensions, block, fluid and fracture properties, injection time and major principal stress, as used for the model validation, were used for these subsequent simulations. A 100 m thick centric pay-zone was created for which the assigned minor principal stress was 80 MPa. Stresses at either side of the pay-zone were same and greater than that of the pay zone, and two different values were considered for them – 85 and 90 MPa. Simulations were performed under three different fluid injection rates – 0.0416, 0.0833 and 0.1666 m^3/s – to investigate their influence on hydraulic fracture propagation under varying in-situ stress states.

Table 1. Properties assigned for block material, hydraulic fracture and fracturing fluid for UDEC simulations.

Block (intact material) properties	
Density (kg/m^3)	2600
Elastic modulus (GPa)	50
Poisson's ratio	0.25
Cohesion (MPa)	25
Friction angle (°)	53
Hydraulic fracture properties	
Cohesion (MPa)	25
Residual cohesion (MPa)	0
Friction angle (°)	53
Residual friction angle (°)	0
Dilation angle (°)	20
Fracture toughness (MPa.m$^{1/2}$)	1.5
Fracturing fluid properties (incompressible)	
Density (kg/m^3)	1000
Viscosity (Pa.s)	0.001

3. Results and discussion

The simulation results for the variations of the length and width of the hydraulic fracture against the injection time under uniform minor principal stress condition (i.e. $\sigma_b = \sigma_a$) along with the corresponding variations derived from the KGD fracture model (i.e. Equations 1 and 2, respectively) are shown in Figure 3.
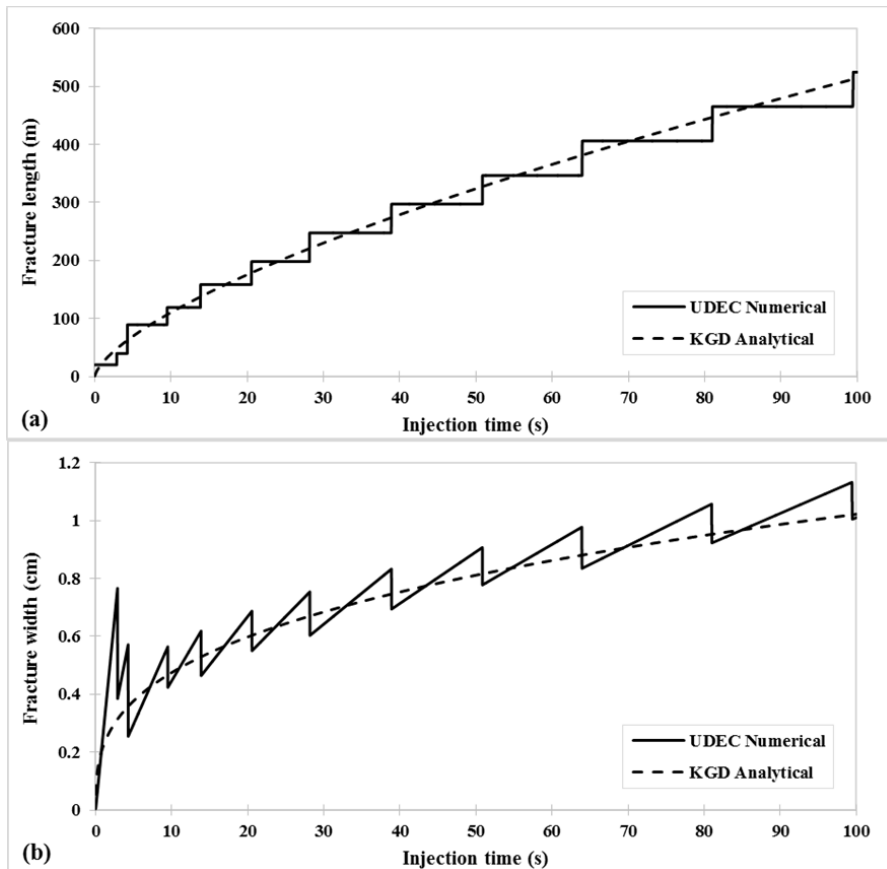
Fig. 3. Numerical and analytical results for hydraulic fracture propagation geometry against injection time under uniform stresses (a) fracture length; (b) fracture width.

Figure 3 displays a good consistency between the numerical results and the corresponding results of the KGD analytical model for the hydraulic fracture geometry meaning that the model is capable of capturing the key mechanics that govern the hydraulic fracture propagation behavior under reservoir conditions.

Variations of the fracture length against the injection time for the simulations performed under the three different injection rates and different stress contrasts are shown in Figure 4.
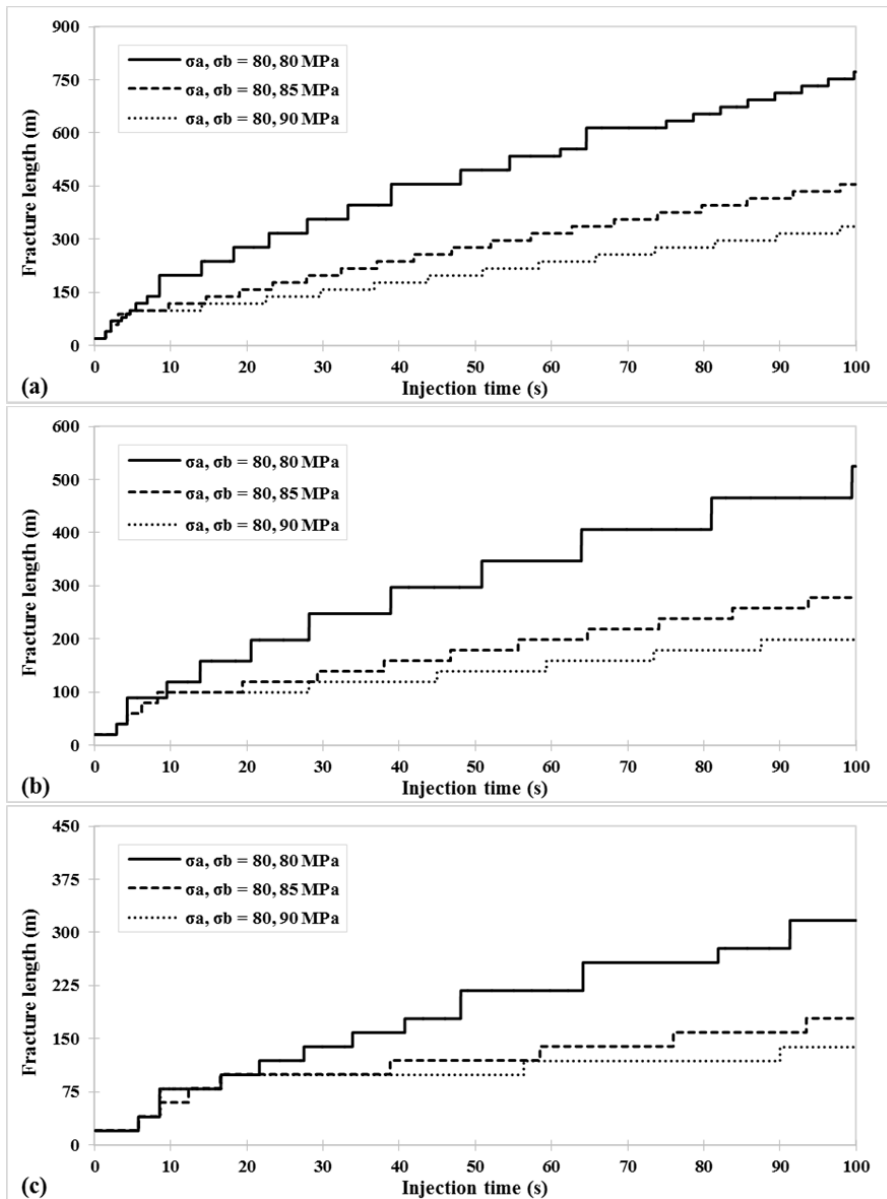
Fig. 4. Fracture length versus injection time for different stress contrasts at injection rate of (a) 0.1666; (b) 0.0833 and (c) 0.0416 m³/s.
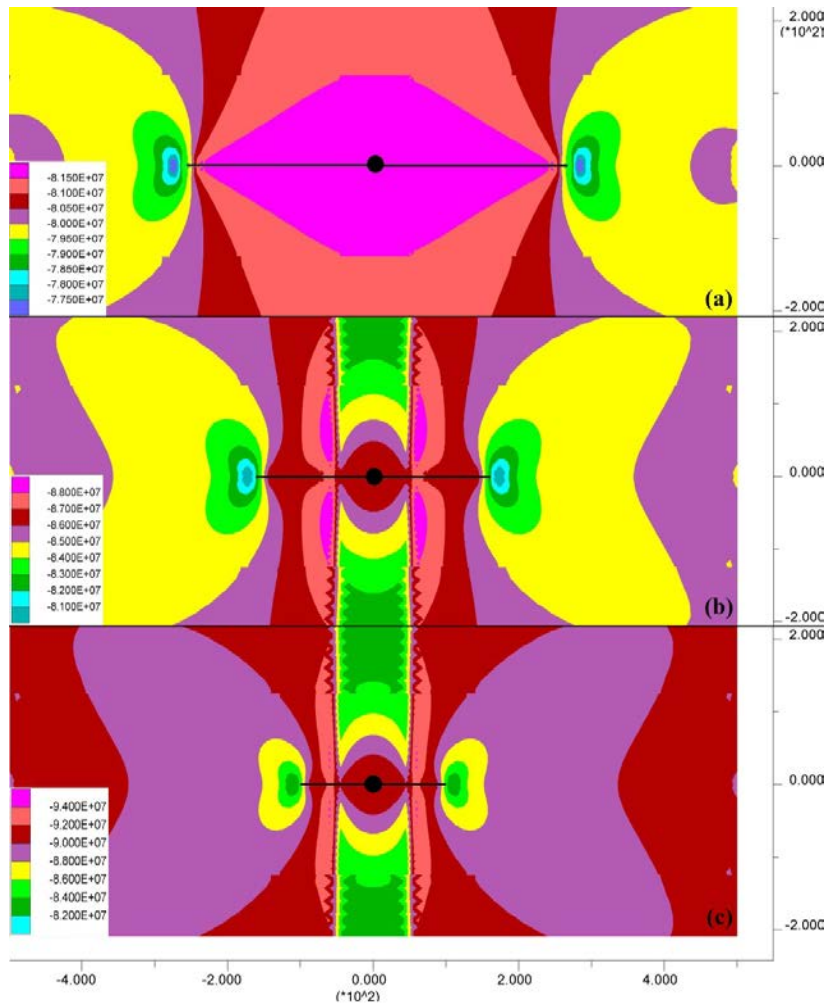
Fig. 5. Positions of hydraulic fractures and minor principal stress distributions after 100 seconds of fluid injection at a rate of rate of 0.0833 m³/s for the stress conditions (a) $\sigma_b = \sigma_a = 80\ MPa$; (b) $\sigma_b = 85$ and $\sigma_a = 80\ MPa$ and (c) $\sigma_b = 90$ and $\sigma_a = 80\ MPa$.

It can be seen from Figure 4 that at each injection rate the first 100 m of the fracture propagation (i.e. until the hydraulic fracture reaches the higher stress zone either side of the wellbore) is similar for both uniform and varying stress conditions. However, the fracture propagation is understandably suppressed by the greater in-situ stress as it enters into the higher-stress zone in the case of the varying stress. In addition, Figure 4 shows that the fracture penetration into the high stress zone is further limited when the stress contrast (i.e. the difference between σ_b and σ_a) is higher as a result of greater resistance to fracture propagation by the acting greater minor principal stress. Figure 5 illustrates the fracture lengths and minor principal stress distribution after 100 seconds of fluid injection at a rate of rate of 0.0833 m³/s for different stress conditions. The phenomenon of decreasing fracture extension due to increasing minor principal stress can be clearly observed from Figure 5.

We plotted the fracture penetration lengths into the higher-stress zone at different injection rates as shown in Figure 6 to delineate the influence of injection rate on the penetration length of the hydraulic fracture under varying in-situ stress conditions.

According to Figure 6, it is clear that increasing injection rate generally increases the length of the hydraulic fractures under all stress conditions. Therefore, the fracture containment by minor principal stress contrast can be more effective under lower injection rates.
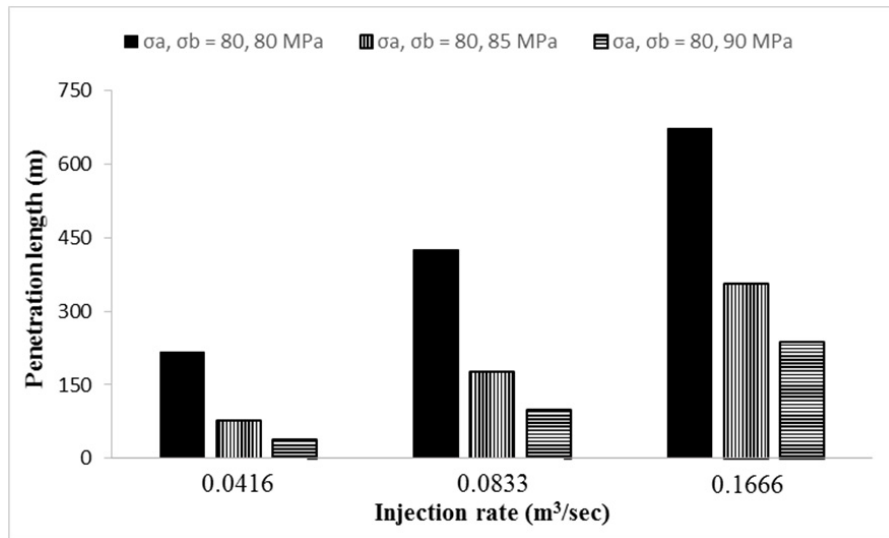

Fig. 6. Hydraulic fracture penetration lengths into the higher stress zone at different injection rates.

4. Conclusions

Hydraulic fracture propagation in deep reservoirs is greatly influenced by the in-situ stress state, which is highly variable in nature due to many factors. A series of numerical simulations using a distinct element method-based software was conducted to investigate the hydraulic fracture propagation behavior under varying in-situ stress conditions. Furthermore, simulations were performed to investigate the effect of fluid injection rate on hydraulic fracture containment behavior.

First, the numerical model was validated assuming uniform in-situ stress conditions. Monitored geometry of propagating hydraulic fracture (length and width) during simulations was compared with those predicted by the KGD analytical fracture model which revealed a good agreement between the two outputs. Then we applied varying stresses perpendicular to the fracture propagating direction (higher stresses were used for bounding zones than for the pay-zone). It was observed that the hydraulic fracture propagation is highly sensitive to the stress contrast between the pay-zone and the bounding zones where greater stress contrasts showed greater propensity for fracture containment. Fluid injection rate also showed a considerable effect on the depth that hydraulic fracture penetrates into the bounding zones. Higher injection rates displayed greater penetrations into the bounding zones. Finally, the results of this study suggest that the natural barriers such as varying stresses, which are very common in reservoirs, effectively restrict the otherwise uncontrollable hydraulic fracture propagation. In addition, operational parameters such as injection rates can be carefully selected to improve the fracture containment by minimizing the fracture propagation into unproductive zones.

Acknowledgements

References

[1] G. Preisig, E. Eberhardt, A. Hosseinian, M. Bustin, Coupled hydromechanical modeling of rock mass response to hydraulic fracturing: Outcomes related to the enhancement of fracture permeability, 13th International Congress of Rock Mechanics (ISRM), Montréal, Canada, 2015.

[2] H. Konietzky, Numerical stress field modelling for underground structures, in: F. Rummel (Ed.), Rock Mechanics with Emphasis on Stress, Oxford & IBH Publishing Co. Pvt. Ltd., New Delhi, 2003, pp. 55–80.

[3] N.R. Warpinski, L.W. Teufel, Influence of geologic discontinuities on hydraulic fracture propagation, J. Petrol. Technol. (1987) 209–220.

[4] A. Agharazi, Determination of maximum horizontal field stress from microseismic focal mechanisms – A deterministic approach, 50th US Rock Mechanics/Geomechanics Symposium, Houston, Texas, USA, (2016) 26-29 June: ARMA, 16–691.

[5] P.L.P. Wasantha, H. Konietzky, Fault reactivation and reservoir modification during hydraulic stimulation of naturally-fractured reservoirs, J Nat. Gas. Sci. Eng. 34 (2016) 908–916.

[6] S.A. Khristianovic, Y.P. Zheltov, Formation of vertical fractures by means of highly viscous liquid, 4th world petroleum congress, Rome, (1955) pp. 579–86.

[7] J. Geertsma, F. de Klerk, A rapid method of predicting width and extent of hydraulically induced fractures, J. Petrol. Technol. 21 (1969) 1571–1581.

[8] T.K. Perkins, L.R. Kern, Widths of hydraulic fractures, J. Petrol. Technol. 13 (1961) 937–49.

[9] R.P. Nordren. Propagation of a vertical hydraulic fracture. Soc. Petrol. Eng. J. 12 (1972) 306–14.

[10] H.A.M. Van Eekelen, Hydraulic fracture geometry: Fracture containment in layered formations. Soc. Petrol. Eng. J. 22 (1982) 341–349.

[11] B.R. Meyer, Design formulae for 2D and 3D vertical hydraulic fractures: model comparison and parametric studies, in: Proceedings of the unconventional gas technology symposium, 1986, pp. 391–408.

[12] C.H. Yew, X. Weng, Fracturing of a wellbore and 2D fracture models, in: Mechanics of Hydraulic Fracturing (2nd Edition), Gulf Professional Publishing, Boston, 2015, pp. 1–22.

[13] J.J. Geertsma, R.R. Haafkens, A comparison of the theories for predicting width and extent of vertical hydraulically induced fractures, J. Energ. Resour.-ASME, 101(1) (1979) 8–19.

[14] E.R. Simonson, A.S. Abou-Sayed, R.J. Clifton, Containment of massive hydraulic fractures. Soc. Petrol. Eng. J. 18 (1978) 27–32.